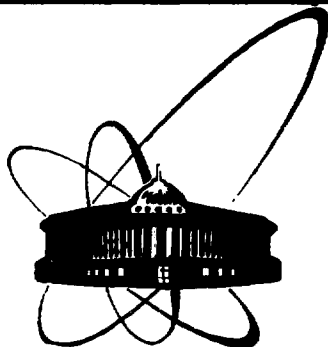


8U9104E39



ОБЪЕДИНЕННЫЙ
ИНСТИТУТ
ЯДЕРНЫХ
ИССЛЕДОВАНИЙ
ДУБНА

E7-89-816

S. A. Karamyan

THE STUDY OF THE ION-CRYSTAL INTERACTION
BY USING THE BLOCKING TECHNIQUE
FOR SCATTERED RECOILS

Submitted to "Nuclear Instruments and Methods"

1989

Introduction

Orientation phenomena are well-known consequences ^{1,2/} of long-range order at the crystal lattice. They influence charged particle motion in the form of crystal channeling and blocking effects. Investigations of the swift heavy ion interaction with single crystals have several aspects:

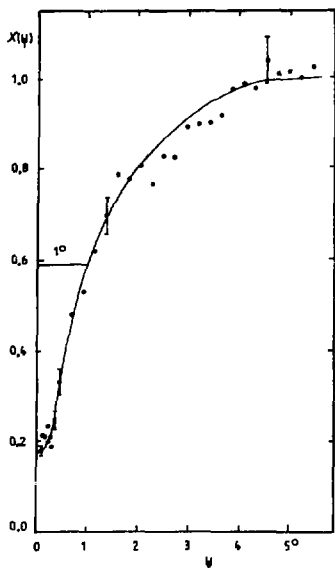
1. The study of the formation mechanism and quantitative parameters of the crystallographic reflections for understanding of dynamical and statistical features of the process.
2. The measurements of the damaging power of swift ions for systematization and clarification of the response of the medium to highly ionizing particle passage.
3. The application of the blocking-effect for measuring the nuclear reaction duration, and advancement in nuclear interaction mechanism.

The experimental method is common for all three aspects.

During many years at the LNR, JINR investigations are being carried out to detect the crystal blocking effect in nuclear reactions induced by heavy ion beams. Experiments have been performed to determine the duration of fission reactions and α -particle emission from excited nuclei, as well as to measure the blocking-effect parameters and radiation damage in the crystals by recording elastically scattered ions.

Recently the method of detecting elastically scattered recoils has proved to be fruitful. The energy-range of recoils is suitable for the observation of crystallographic reflections in the wide range of projectile energies, (0.1-100) MeV/amu. In addition, the emission angle of recoils is convenient for registration over a wide range of projectile masses, both smaller and larger ones than the target mass.

Solid state track detectors have integrating, threshold and position-sensitive properties, and are used successfully for recording crystallographic reflection patterns. Quantitative measurements of reflection parameters are carried out by scanning detectors with an optical microscope and by measuring the track density as a function of coordinate. In fig. 1 the blocking-minimum profile is exhibited, for example, in the case of registering the recoils (C), emitted from diamond. As a result of a large number of experiments, data are collected on the blocking-effect parameters as a function of the atomic number and energy of the nuclei detected, and of the active layer thickness



for different crystals. Here presented are the results of an experimental study, using the given method, of three essential problems connected with orientation effects formation, ion-induced crystal damages, and nuclear lifetime estimation.

Fig. 1. Profile of the axial $\langle 101 \rangle$ blocking minimum measured in diamond irradiation with ^{129}Xe (122 MeV) ions and in recoils (C) registration at the angle $\theta_L = 74^\circ$ to the beam.

I. Volume Capture of Nuclei to Channeling

There is a general view that in recording the angular distribution of particles scattered at large angles one should observe the blocking effect. But in our experiments with Ge crystals a transformation of crystallographic reflections is displayed ^{/5/} with a variation of detection angle θ_L . As θ_L decreases in the range $\theta_L = 80-30^\circ$, the inversion of contrast blocking minima to the channeling maxima takes place. Later this fact was explained qualitatively ^{/4/} by an increase in the target active layer thickness in terms of the secondary capture to channeling of the particles going out from the depth of the crystal. In papers ^{/5,6/} an analogous effect is observed in the bombardment of silicon and diamond single crystals by different heavy ions. A summary of these results is presented below.

A few words about the experimental conditions. Polished, (111) or (110) oriented wafers $\lesssim 1$ mm thick made from monocrystalline high-quality diamond, Si and Ge are used as targets. They are bombarded by heavy ion beams with energies from 0.4 to 6 MeV/amu at the U-300

cyclotron. After passing a collimator the beam had the following parameters: an angular spread of $<0.5^\circ$, a diameter of 1 mm (on target), an intensity of $<2 \times 10^{10} \text{ s}^{-1}$, and pulsed power of $<1 \text{ W}$. Irradiations were carried out under nonaligned conditions at room temperature. The beam-induced temperature rise on the targets mounted on a metallic backing was insignificant. The crystal damage can be neglected at the dose required for recording the reflection pattern.

Scattered ions and recoil nuclei were detected with a glass track detector, as well as with plastics (cellulose nitrate and polyethylene terephthalate), covered by an Al foil and without it. Hence the reflection pattern can be recorded separately for scattered ions and for recoil nuclei. The glass detector had a threshold of registration of about 5 MeV in energy and $Z \approx 10$ in the atomic number of the particle, the plastics had much lower detection thresholds. The visualization of the pattern is achieved by the chemical development of the tracks (provided the track density is sufficiently high).

Pattern photographs are displayed in fig. 2. They are taken during the exposures ^{15/} of a Si crystal to ^{40}Ar ions with energies of 25 MeV (a) and 151 MeV (b). In the latter case the inversion of the blocking to channeling pattern is obvious. The relative yield X_0 of recoils along the $\langle 111 \rangle$ Si axis is shown in fig. 3 as a function of the ^{40}Ar energy. The transition from blocking to the channeling effect and retrogression to blocking again with energy growth are evident.

This complex behaviour is connected with the creation, at the intermediate beam energy, of the conditions which are analogous to a "buried" source of elastic recoils. This results from the two factors: first, the drastic variation of the elastic recoil kinetic energy with angle: $E_{rn} \sim \cos^2 \theta_L$, which leads to a change in the target active layer, t ; and second, the energy dependence of the inelastic-elastic cross section ratio.

This kind of secondary channeling patterns was observed in many other interactions, for instance, in ^{129}Xe (122 MeV) on Si and diamond in the angle range of $30-40^\circ$, and in the reaction ^{20}Ne (104 MeV) + Ge at $\theta_L = 40-60^\circ$. The latter case is illustrated by fig. 4. The scattered Ne ions were detected by polyethylene terephthalate covered by an Al foil in order to discriminate the recoils. Planar and axial channeling maxima were found.

A high-quality blocking pattern was observed in the (θ_L, E_L) region, where active thickness $t \lesssim 2 \mu\text{m}$ (along the detection direction), in contrast to the channeling maxima seen for a thickness of up to $5-10 \mu\text{m}$. The last value is probably the minimum layer necessary for the trans-

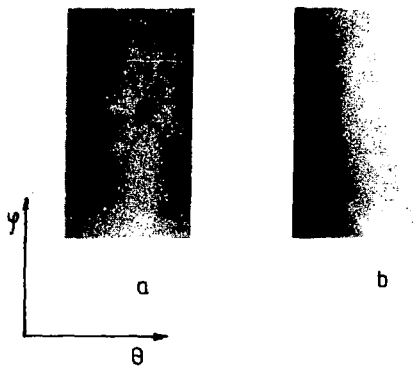


Fig. 2. Reflection patterns recorded with glass detectors in the exposure of a silicon crystal to ^{40}Ar ions with energies of 25 MeV (a) and 151 MeV (b).

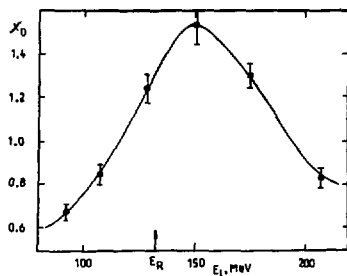


Fig. 3. Relative yield X_0 of recoils along the Si $\langle 111 \rangle$ axis, oriented at 53° to the ^{40}Ar beam, as a function of projectile energy. E_R is the grazing energy.

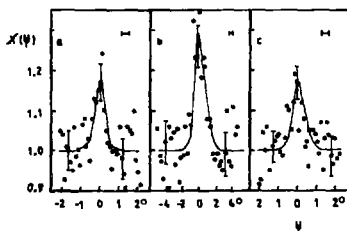


Fig. 4. Reflection profiles for ^{20}Ne ions scattered in the Ge directions $(11\bar{1})$, $\langle 111 \rangle$ and $(01\bar{1})$ oriented at angles 52° (a), 58° (b) and 55° (c) relative to the beam.

formation of the blocking-type angular distribution to the secondary channeling one. In the case of fission fragment interaction with heavy crystals (W, UO_2) no similar channeling pattern was observed. This is explained in terms of the expansion of blocking phase-volume for fission fragment trajectories on heavy crystals.

Thus the volume capture of medium-weight nuclei to channeling in diamond, Si, and Ge crystals has been established experimentally. Capture to channeling was discussed ^{17/} extensively for high-energy proton interactions with monocrystalline media. Such processes are particular cases of the general property of complex mechanical systems, known as spontaneous transition from chaotic motion to the ordered one.

II. Damaging Power of Swift Heavy Ions

Now a growing interest is being shown in high-energy ion implantation. Some new possibilities of creating vertical device structures and other applications are exhibited ^{18,9/} in silicon implantation. Also, the crystal damage process induced by highly ionizing ions is important in the physical sense.

By using the crystal-blocking technique the damaging power of ions from Ne to Xe for diamond, Si and Ge crystals has been studied in the energy range 10-130 MeV. The experimental method was the same as described above. The blocking effect was detected for elastically scattered ions and recoils. The condition of a thin ($\leq 2 \mu m$) target active layer was satisfied. Contrast blocking minima ($X_0 \leq 0.4$) are observed for every crystal-projectile case at the beginning of irradiation. The intensity of the blocking effect was attenuated with growing ion fluence Φ , the minimum yield X_0 increased and tended to 1 at crystal amorphization. Thus ion-induced damage was controlled on the surface layer of the crystal with a thickness much smaller than the projective range of ions.

The measured values of the minimum yield $X_0(\Phi)$ are transformed to $X_{rad}(\Phi)$ according to the formula:

$$X_{rad}(\Phi) = 1 - [1 - X_0(\Phi)] [1 - X_0(0)]^{-1} \quad (1)$$

The quantities $X_{rad}(\Phi)$ correspond to the radiation damage effect, $X_0(0)$ refers to a non-irradiated crystal. The damaging power parameter $\Delta X_{rad}/\Delta \Phi = 0.1/\Phi_{0.1}$ characterises the degree of disorder per dose unit in a unified way.

In fig. 5 experimental results are shown for Ar and Xe ion interactions with a diamond crystal. The damage effect as well as the unexpectedly low damaging power of Xe ions relative to Ar are obvious.

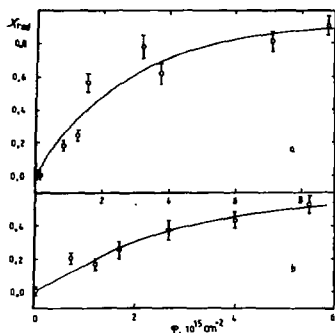


Fig. 5. The yield X_{rad} in the blocking minimum $\langle 101 \rangle$ of diamond versus ion fluence: 25 MeV ^{40}Ar (a) and 122 MeV ^{129}Xe (b).

It is reasonable to look for the correlation of the measured damaging power with the parameters of nuclear and electronic energy loss of ions. In the projectile energy range E_L 0.5 MeV/amu dispersed defects are generated in random events of nuclear collisions. Hence the cross section of defect formation can be calculated by integrating the angular distribution of scattered recoils by taking into account the defect multiplication per primary recoil. The following formula was derived:

$$\sigma_D(\text{cm}^2) = \frac{3.62 \cdot 10^{-13} a Z_1 Z_2 \gamma}{E_d (1 + \gamma)} \int_{\theta_{\min}}^{\theta_{\max}} f(t^{1/2}) d\theta + \frac{2.60 \cdot 10^{-26} Z_1^2 Z_2^2 \gamma}{E_d E_L}, \quad (2)$$

where $\gamma = A_1/A_2$, a is the Thomas-Fermi screening parameter, E_d is the displacement energy of an atom, and $f(t^{1/2})$ is the universal scattering function. The realistic scattering cross section was taken from ref.^{10/}

The systematics of damaging power as a function of the calculated σ_D values is presented in fig. 6. The data on Si and Ge crystals are included. It is seen that all points lie on a linear function except the results for Xe ions. Hence the correlation of the damaging power with the cross section σ_D is corroborated, but a new mechanism, attenuating the defect formation, is valid for very heavy ions (e.g. Xe). This anomaly was observed earlier^{11-13/} and interpreted as the self-annealing of each ion track provided the energy-release density was sufficiently high.

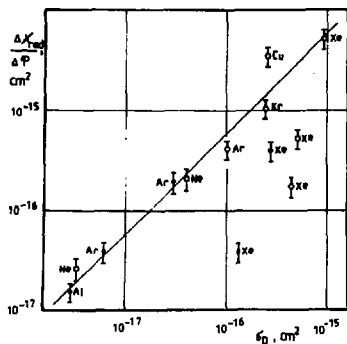


Fig. 6. Correlation between the ion damaging power and the calculated cross section σ_D of defect formation. Black point refers to Si crystal, light one to Ge.

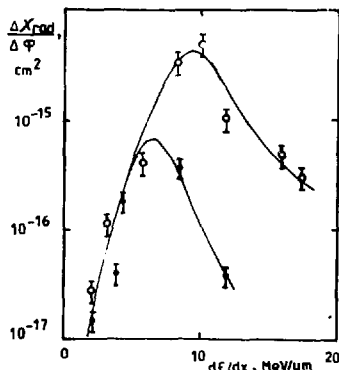


Fig. 7. The same as in fig. 6, in correlation with the electronic stopping power of ions.

Then the correlation between the damaging power and electronic stopping power dE/dx should be important. It is plotted in fig. 7. Indeed, the threshold activation of the new mechanism of crystal media response is confirmed for high dE/dx values. In fig. 7 the growth changes to retrogression at the threshold whose value is different for Si and Ge, possibly, because of the difference in the diffusion coefficients of atoms in the two materials.

The model which identifies the defects with the atoms displaced in nuclear collisions does not explain the Xe anomaly, nor the ratio between the radiational resistance of diamond and Ge. Another model which is valid for dielectrics considers the Coulomb ion-explosion as a reason for the destruction of volumes (latent track formation). It predicts the amorphization of diamond for the fluence values of about 10^{12} cm^{-2} . In fact, the long-range order in diamond remains for a fluence of up to 10^{15} cm^{-2} . Hence this model is also incapable of reproducing the crystal behaviour. A more complicated nature of the crystal media response to a highly ionizing particle is revealed.

III. Influence of the Nuclear De-Excitation Time on the Blocking Minimum

Blocking-reflection formation has some peculiarities in the case of the registration of inelastic nuclear reaction products. As known, not only the perfection of the lattice, but also the displacement of the product emission point play an important role. Excited products decay by the emission of α -particles and nucleons, and γ -rays produce recoil momentum with the additional angular spread which changes the trajectory of the product in monocrystalline medium. The influence of the de-excitation process on the blocking minima was revealed experimentally in papers /3,5,14,15/.

The registration of energetic nuclei with solid state track detectors provides the possibility of selective detection of target-like products. This method was used for measuring /15/ the blocking minimum yield X_0 as a function of ion energy in the reactions $^{20}\text{Ne} + \text{Ge}$ and $^{22}\text{Ne} + \text{Ge}$. The results are exhibited in fig. 8. It is evident that with an ion-energy growth the absolute yield of detected products decreases as a consequence of the degrading of elastic and quasielastic processes, and the relative yield X_0 increases because of the de-excitation effect. Hence the de-excitation time is estimated to be 1.5×10^{-16} s.

If a target-like product is emitted at the angle θ_L in the lab. system, then the total excitation energy of binary reaction products is restricted /3,5/ by kinematical limit $E^* \leq E_{\text{lim}}^*$:

$$E_{\text{lim}}^* = \frac{E_L}{A_1 + A_2} \left(A_2 - \frac{A_1 A_4}{A_3} \sin^2 \theta_L \right) + Q, \quad (3)$$

where $A_1 \dots A_4$ are the mass numbers of reaction participants, and Q is the energy release in the reaction. Hence the excitation energy of products increases with projectile energy E_L , but does not exceed the E_{lim}^* value. So it is possible to choose, by varying θ_L , the mean excitation energy of a target-like product near the threshold of strong decay.

De-excitation near threshold takes time about equal to the electromagnetic decay period of 10^{-16} s. Consequently this long delay has to influence the blocking minimum in a pronounced way. This is the case /5/ for the reactions of ^{27}Al and ^{40}Ar with silicon crystals, as shown in fig. 9.

Particle emission from the product simulates the displacement S of its trajectory from the atomic row:

$$S = v_4 \tau_4 \sin \bar{\theta}, \quad (4)$$

Fig. 8. The relative yield χ_0 at the minimum measured for the reactions $^{20}\text{Ne}+\text{Ge}$ and $^{22}\text{Ne}+\text{Ge}$ as a function of projectile energy. The absolute reaction yield Y , and displacement S are also shown. The dashed line is a guide one for the points χ_0 and Y , the solid line indicates the S values.

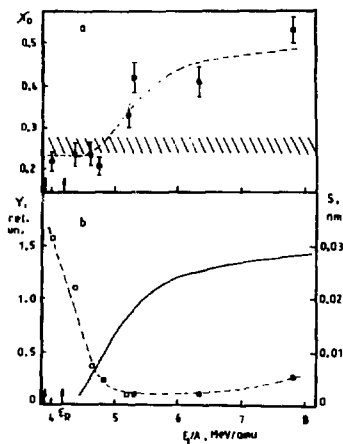
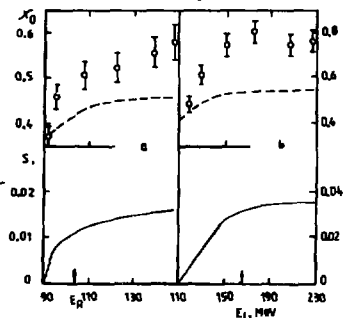


Fig. 9. Yield χ_0 and displacement S versus projectile energy for reactions $^{27}\text{Al} + \text{Si}$ (a) and $^{40}\text{Ar} + \text{Si}$ (b). Points are results of measurements, dashed line is the contribution of the electromagnetic decay period to χ_0 , the solid line indicates the S values.



where V_4 and τ_4 are the laboratory velocity and the lifetime of a target-like product, respectively, and $\bar{\theta}$ is the mean angle of deflection created by the recoil of particle emission. If $V_4\tau_4 \gg d$, where d is the interatomic distance, the displacement S becomes unimportant because the angular distribution of blocking is formed before particle emission. However, the angular spread still influences the blocking reflection in the same manner as the angular resolution does.

For the reactions $^{27}\text{Al} + \text{Si}$ and $^{40}\text{Ar} + \text{Si}$ (fig. 9), the strong decay lifetime generates the displacements, and electromagnetic decay creates the angular dispersion $\Delta\psi$:

$$\Delta\psi \sim \bar{E}_\gamma M_8^{1/2}, \quad (5)$$

where \bar{E}_γ and M_8 are the mean energy and multiplicity of a γ -ray cascade, respectively. The contribution from electromagnetic decay was simulated numerically and the displacement S , connected with the lifetime of strong decay, τ_4 , was extracted, as shown in fig. 9.

Finally, the lifetime of Si nuclei is determined to be $(2-4) \times 10^{-17}$ s for the mean excitation energy near the threshold of particle emission. These values do not contradict the tabular data /16/.

Thus, a variant of the experimental estimation of the de-excitation time for inelastic nuclear collision products has been worked out on the basis of the crystal-blocking technique. In ion-crystal bombardments new information is also obtained about the mechanism of reflection formation during the passage of excited or unexcited nuclear products, and about the regularities and anomalies in the ion damaging power.

The author gratefully acknowledges the help of his colleagues, the co-authors of papers /6,11-13/.

Recently at the São Paulo Nuclear Physics Conference Italian and South African groups reported some results /17,18/ which confirm ours on the blocking effect observed /5/ for inelastic collision products in a Si single crystal.

References

1. Lindhard, J. K. Dan. Vidensk. Selsk. Mat.-Fys. Medd., 1965, v.34, no.14.
2. Gemmell, D.S. Rev. Mod. Phys., 1974, v.46, p.129.
3. Karamyán, S.A. Pisma Zhurn. Exper. Teor. Fiz., 1984, v.40, p.196.
4. Karamyán, S.A. Izv. AN SSSR, ser.fiz., 1987, v.51, p.1008.
5. Karamyán, S.A. Yad. Fiz., 1989, v.49, p.934.
6. Didyk, A.Yu., Zaitsev, A.M., and Karamyán, S.A. JINR Rapid Communications, 1989, no.4(37), Dubna.
7. Andreev, V.A., Baublís, V.V., Damaskinski, E.A. et al. Pisma Zhurn. Exper. Teor. Fiz., 1982, v.36, p.340.
8. Proceed. Intern. Conf. on Ion Implantation. Nucl. Instr. & Meth., 1989, v.B37/38.
9. "Ion Implantation and Beam Technology" Academic Press, Sidney, 1984.
10. Wilson, W.D., Haggmark, L.G., and Biersack, J.P. Phys. Rev., 1977, v.B15, p.2458.
11. Karamyán, S.A., Rykhliuk, A.V., and Bugrov, V.N. JINR Rapid Communications, 1987, no.5(25), Dubna.
12. Karamyán, S.A., Oganessian, Yu.Ts., and Bugrov, V.N. Nucl. Instr. & Meth., 1989, v.B43, p.153.
13. Bugrov, V.N., and Karamyán, S.A. Preprint JINR, Pt4-89-681, Dubna, 1989.
14. Gomez del Campo, J., Shapira, D., Biggerstaff, J.A. et al. Phys. Rev. Lett., 1983, v.51, p.451.

15. Karamyán, S.A. *Yad. Fiz.*, 1987, v.46, p.1338.
16. Endt, P.M., and Van der Leun, C. *Nucl. Phys.*, 1978, v.A310, p.1.
17. Boccaccio, P., Bracco, A., Fioretto, E. et al. *Proc. Intern. Nucl. Phys. Conf. São Paulo*, 1989, v.1, p.283.
18. Fearick, R.W., Hoernle, R.F.A., and Sellachop, J.P.F. *ibid*, p.329.

Received by Publishing Department
on December 8, 1989.

SUBJECT CATEGORIES OF THE JINR PUBLICATIONS

Index	Subject
1.	High energy experimental physics
2.	High energy theoretical physics
3.	Low energy experimental physics
4.	Low energy theoretical physics
5.	Mathematics
6.	Nuclear spectroscopy and radiochemistry
7.	Heavy ion physics
8.	Cryogenics
9.	Accelerators
10.	Automatization of data processing
11.	Computing mathematics and technique
12.	Chemistry
13.	Experimental techniques and methods
14.	Solid state physics. Liquids
15.	Experimental physics of nuclear reactions at low energies
16.	Health physics. Shieldings
17.	Theory of condensed matter
18.	Applied researches
19.	Biophysics

Карамян С.А.

E7-89-816

Изучение взаимодействия ионов с кристаллами
с помощью эффекта теней для ядер отдачи рассеяния

Приведены экспериментальные данные по наблюдению ориентационных эффектов при облучении монокристаллов алмаза, Si и Ge быстрыми тяжелыми ионами и регистрации ядер отдачи рассеяния. Впервые обнаружен и изучен объемный захват средних ядер в режим каналирования. Систематизирована повреждающая способность ионов и установлено ее аномально низкое значение для ионов Xe. Обсуждается механизм отрыва кристаллической среды на прохождение высокоионизирующей частицы. Описан вариант экспериментальной оценки времени девозбуждения продуктов неупругих столкновений ядер на основе эффекта теней.

Работа выполнена в Лаборатории ядерных реакций ОИЯИ.

Препринт Объединенного института ядерных исследований. Дубна 1989

Karamyan S.A.

E7-89-816

The Study of the Ion-Crystal Interaction
by Using the Blocking Technique
for Scattered Recoils

Experimental data are presented on the orientation effects observed in the swift heavy ion exposures of diamond, Si and Ge crystals by recording recoil nuclei. The volume capture of medium-weight nuclei to channeling has first been revealed and studied. Ion damaging power is systematized and the anomalously low damaging power of Xe ions is established. The crystal media response to the passage of highly ionizing particles is discussed. On the basis of the crystal-blocking technique a variant of the experimental estimate of the de-excitation time for inelastic collision products is described.

The investigation has been performed at the Laboratory of Nuclear Reactions, JINR.

Preprint of the Joint Institute for Nuclear Research. Dubna 1989

16 коп.

Редактор Э.В.Ивашкевич. Макет Р.Д.Фоминой.

Подписано в печать 15.12.89.
Формат 60х90/16. Офсетная печать. Уч.-изд.листов 1,07.
Тираж 335. Заказ 42904.

Издательский отдел Объединенного института ядерных исследований.
Дубна Московской области.